Structural Interactions between *n*-Paraffins and Their Perdeuterated Analogues: Binary Compositions with Identical Chain Lengths

Douglas L. Dorset

Electron Diffraction Department, Medical Foundation of Buffalo, Inc., 73 High St., Buffalo, New York 14203

Received May 20, 1991; Revised Manuscript Received July 23, 1991

ABSTRACT: Electron diffraction and calorimetric studies were made on perdeuterated *n*-paraffins and compared to the fully hydrogenated analogues. It is seen that the crystal structures of the respective molecules are identical with no *measurable* difference seen between their unit cell dimensions. As shown earlier, the incorporation of deuterium does not greatly change the molar transition enthalpy of the molecules. However, for a homologous series, perdeuteration lowers the chain length where the transition to a "rotator" phase vanishes. Otherwise, the chain disorder for the analogous compounds is identical when they are heated. Binary phase diagrams of equal chain length compositions are not only ideal for the phase boundary between the "rotator" phase and the melt, as found for all cosoluble *n*-paraffins, but also for the orthorhombic to "rotator" transition. These observations suggest that the dispersion forces for the two chemical species are very similar.

Introduction

Perdeuterated or partially deuterated polymethylene chains have often been employed as (presumably) nonperturbative probes of *n*-alkane chain packing for many types of molecular systems. In membrane biophysics, selectively deuterated polymethylene segments used in neutron diffraction experiments on phospholipid multilamellar arrays allowed carbon atom positions in acyl chain and headgroup moieties to be located in order to facilitate description of the molecular conformation.[1,2] Selectively deuterated alkanes have been employed in vibrational spectroscopic studies of defect content in heated samples[3] or in molecular mixtures of a lamellar solid solution.[4] In polymer science, perdeuterated polyethylene adducts were used to seek the presence of adjacent reentry for crystals grown from solution or the melt, both by vibrational spectroscopy[5-7] or neutron diffraction.[8-10]

In model studies relevant to polymer science, the assumed random molecular mixing in non-chain-folded binary combinations of deuterocarbon with hydrocarbon has been questioned,[11] a result which could also affect the interpretation of data from chain-folded polyethylene lamellae. Theoretical calculation of a critical temperature for phase separation[12] shows a molcular weight dependence for fractionation which would be important for polymer lamellae. On the other hand, this perturbation was not expected to be significant for the alkanes. Nevertheless, the melting point difference between a paraffin and its perdeuterated analogue was thought to lead to molecular clustering in the binary solid state, since a heterogeneous composition of the two ingredients is implied by the finite separation of the liquidus and solidus curves in the solid solution phase diagram.[11] Counterarguments were made,[13] maintaining that, for the low perdeuterated probe concentrations used, a random distribution of chains was maintained despite the compositional heterogeneity. Neutron diffraction experiments on such solids support the postulated random mixing.[9] Later evaluation of binary phase diagrams for n-$C_{36}H_{74}$/n-$C_{36}D_{74}$ and polyethylene/polyethylene-d_4 finds no evidence for phase separation, even for the binary polymeric solid,[14] although a measurable compositional heterogeneity exists at intermediate concentrations. On the other hand, numerous reports of phase separation for noncrystalline polymeric binary combinations, where one component differs from the other only by replacement of all hydrogens by deuterium,[15] have been published.

There is very little detailed structural work published on the interaction of *n*-alkanes with isotopically substituted analogues. This paper reports a crystallographic and calorimetric study of *n*-paraffins and respective deuterium-substituted compounds, both as pure molecular crystals and as crystalline combinations of two analogous compounds having identical chain lengths. This study, moreover, serves as a control for work to be reported later, which describes the occurrence of significant isotope effects in binary compositions with unequal chain length.

Materials and Methods

***n*-Paraffins.** The perprotonated *n*-paraffins used in this paper were purchased from sources listed in Table I and are generally greater than 97% pure. The analogous perdeuterated *n*-paraffins are of comparable or greater purity and were purchased from MSD Isotopes. Other paraffins used for heating experiments in the electron microscope are described in an earlier paper[16] except for n-$C_{82}H_{166}$, which was a gift from Dr. J. R. Fryer, and has thermal properties given by Broadhurst.[17] Crystallization of the solid paraffins and their fused binary combinations was carried out either from solvent or epitaxially on benzoic acid, using procedures described earlier.[18] The former crystallization affords a view down the molecular long-chain axis whereas epitaxial orientation produces an orthogonal view onto the chain axes.

Electron Diffraction. Selected-area electron diffraction experiments were carried out at 100 kV either with a JEOL JEM 100B7 or a JEM 100CXII electron microscope, operating under typical low beam dose conditions to ensure that the crystalline specimens were protected against significant radiation damage.[18] Patterns were photographed on Kodak DEF-5 X-ray film to permit a fast recording time at a useful camera length at such low beam currents. Heating experiments were performed with a GATAN 626 specimen stage which can maintain any temperature between −170 and +150 °C. For quantitative crystal structure analysis, kinematical scattering was assumed under the conditions defined previously for such specimens.[19] Unit cell constants were calibrated with gold Debye–Scherer patterns photographed at the same lens settings used to record the paraffin diffraction patterns.

Calorimetry. Differential scanning calorimetric measurements were made with a Mettler TA3300 instrument with a liquid nitrogen cooled cell, permitting measurements down to −170 °C,

0024-9297/91/2224-6521$02.50/0

Table I
Thermal Data for Pure Alkanes and Perdeuteroalkanes

compound	source[a]	purity, %	temp, °C				heat of fusion, kcal/mol	
			T_p[b]	lit.	T_m[b]	lit.	ΔH_f[b]	lit.
n-$C_{19}H_{40}$	1	97	21.7	22.8	31.6	32.1	15.8	14.3
n-$C_{19}D_{40}$	2	99.6	19.8	–	27.7	–	13.2	
n-$C_{20}H_{42}$	3	>99			36.6	36.8	16.5	16.8
n-$C_{20}D_{42}$	2	98.7			33.6	–	14.7	
n-$C_{24}H_{50}$	1	97	47.8	48.1	50.9	50.9	21.0	20.6
n-$C_{24}D_{50}$	2	99.7	45.6	–	46.6	–	19.7	
n-$C_{30}H_{62}$	3	99	63.0	62.0	66.1	65.8	26.3	
n-$C_{30}D_{62}$	2	99.2	60.7	–	61.8	–	22.3	
n-$C_{32}H_{66}$	4	98.3	67.2	–	69.5	68.7	27.2	
n-$C_{32}D_{66}$	2	>99	63.2	–	65.6	–	23.6	
n-$C_{36}H_{74}$	3	>99	74.4	73.8	76.5	76.2	31.6	28.5
n-$C_{36}H_{74}$	2	98			72.5	71.6	28.7	

[a] (1) Aldrich (Milwaukee, WI); (2) MSD (Montreal, Quebec); (3) Supelco (Bellefonte, PA); (4) Eastman (Rochester, NY). [b] Legend: T_p, premelt transition temperature; T_m, melting temperature; $\Delta H_f = \Delta H_p + \Delta H_m$.

operating at highest sensitivity, and scanning samples sealed in aluminum crucibles (minimal weight of 0.5 mg). Transition enthalpies ΔH were calibrated against the known value for indium and the calorimeter temperaure scale calibrated by a linear fit to the previously reported bulk melting points for the perprotonated paraffins.[20] In plots of binary phase diagrams, only peak temperatures were used. Peak melting temperatures for pure components are given in Table I along with ΔH values.

Calculations of solid solution melting temperature were made assuming Raoult's law behavior, using expressions derived by Lee.[21] Since we plot peak transitions, an average is made of the calculated liquidus (L) and solidus (S) curves to compare with this peak temperature. Hence, the mean mole fraction $x_B = {}^1/_2(x_B^{(L)} + x_B^{(S)})$ is used, where

$$x_B^{(S)} = (e^{-A} - 1)/(e^{-A} - e^{B})$$

and

$$x_B^{(L)} = e^{-B} x_B^{(S)} \qquad (1)$$

This is based upon the definitions:

$$e^{-A} = \exp\left[-\frac{\Delta H_A}{R}\left(\frac{1}{T} - \frac{1}{T_A}\right)\right]$$

and

$$e^{-B} = \exp\left[-\frac{\Delta H_B}{R}\left(\frac{1}{T} - \frac{1}{T_B}\right)\right]$$

Results

Pure Perdeuteroparaffins. Electron diffraction patterns from perdeuterated n-$C_{30}D_{62}$, n-$C_{32}D_{66}$, or n-$C_{36}D_{74}$ in projections down the chain axes (solution crystallization) or onto the chain axes (epitaxial crystallization) are identical in appearance to those from the perprotonated n-paraffins (Figure 1). For the epitaxially oriented crystals, indices of the most intense reflections in $0kl$ patterns are seen again to be simply related to the carbon number of the chain n-C_mD_{m+2}, as shown before for even-chain n-paraffins in the orthorhombic space group $Pca2_1$, i.e for $01l$, $l = m, m+2$, for $00l$, $l = 2m+2, 2m+4$. Lattice constants for the lamellar repeat direction are virtually identical to the values determined for analogous n-paraffins.[22,23] (Table II shows two examples.)

In the view down the chain axes, it also is not possible to distinguish the lattice constants for the lateral chain packing of perdeuteroalkanes from those of the corresponding n-paraffins (Table II). Quantitative structure analysis of the chain layer packing was carried out using $hk0$ electron diffraction intensities from lozenge-shaped monolamellar crystals of two deuterium-substituted paraffins. The structure factors calculated from the accepted

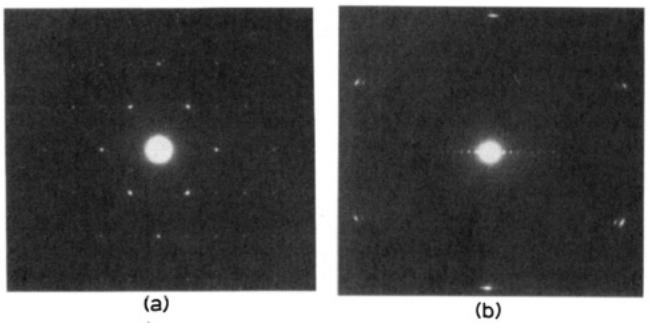

Figure 1. Electron diffraction patterns from the perdeuterated n-paraffin n-$C_{36}D_{74}$: (a) solution crystallized, projection down chain ($hk0$) pattern); (b) epitaxially crystallized, projection onto chains ($0kl$) pattern. (The patterns are not shown at the same scale.)

Table II
Crystallographic Data for Two n-Paraffins and Their Perdeuterated Analogues

compound	unit cell axes, Å			
	a	b	c	c (lit.)
n-$C_{30}H_{62}$	7.58 ± 0.07	5.06 ± 0.03	41.0 ± 0.4	40.0[a]
n-$C_{30}D_{62}$	7.57 ± 0.06	5.05 ± 0.02	41.3 ± 0.3	–
n-$C_{36}H_{74}$	7.59 ± 0.07	5.05 ± 0.03	48.1 ± 0.6	47.6[a]
n-$C_{36}D_{74}$	7.56 ± 0.03	5.01 ± 0.03	48.8 ± 0.3	–

[a] Reference 36.

methylene chain packing for the $0_\perp$ subcell fit the observed data very well (Table III), i.e. within the accuracy normally found for electron crystallographic analyses of polymethylene compounds.[22]

DSC scans of the n-paraffins and their perdeuterated analogues were used to measure peak transition temperatures. When a comparison is possible, the values measured are similar to those determined earlier.[11,14,16,20,24] It also will be noted from Table I that the melting points of the deuteroalkanes are consistently lower than those of the respective perprotonated compound. The melting behavior can be understood in terms of the law of corresponding states. As described previously,[25] when melting point differences of linear chains from methane to polyethylene are plotted against melting point of the hydrocarbon, the slope found is very close to the value δ determined by Grigor and Steele[26] in their study of isotope effects on the methane triple point.

We also note that the orthorhombic to hexagonal ("rotator phase") transition temperature for deuteroalkanes is somewhat lower than that of the corresponding hydrogenated n-paraffin (Figure 2). Moreover, the interval

Table III
Electron Diffraction Structure Analyses for Two Perdeuteroalkanes Based on the Crystal Structure of n-$C_{36}H_{74}$[22,a]

$hk0$	$\|F_{calc}\|$	$\|F_{obs}\|$	$hk0$	$\|F_{calc}\|$	$\|F_{obs}\|$
		n-$C_{30}D_{62}$ (R = 0.14)			
200	1.96	1.90	120	0.39	0.38
400	0.90	0.82	220	0.40	0.56
110	2.06	2.00	320	0.48	0.43
210	0.43	0.51	420	0.19	0.36
310	0.63	0.88	130	0.62	0.47
410	0.34	0.43	230	0.47	0.33
510	0.35	0.34	330	0.22	0.25
020	1.20	1.04	430	0.42	0.34
		n-$C_{36}D_{74}$ (R = 0.18)			
200	2.27	1.80	320	0.56	0.62
400	1.04	0.89	420	0.22	0.46
110	2.38	1.94	520	0.50	0.49
210	0.49	0.57	130	0.71	0.63
310	0.73	0.86	230	0.55	0.52
410	0.40	0.52	330	0.26	0.39
510	0.40	0.46	430	0.48	0.48
610	0.34	0.29	040	0.28	0.25
020	1.38	1.32	140	0.32	0.32
120	0.45	0.54	240	0.06	0.20
220	0.46	0.76	340	0.43	0.39

[a] Deuterium electron scattering factor assumed to be identical with that of hydrogen. Structure factors are relative values.

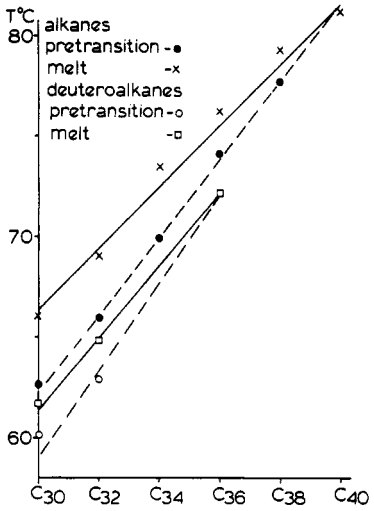

Figure 2. Plot of melting points and premelting temperatures for n-paraffins and their perdeuterated analogues.

between "rotator" transition and melting temperature narrows for the orthorhombic series. (This transition is found for n-$C_{36}D_{74}$ only when the samples are crystallized from the melt.[11,14]) Thus, deuterium substitution of an n-paraffin lowers the chain length for which the premelt transition *disappears* by about four carbon atoms.

In earlier studies,[11,14] the molar enthalpies of fusion for the hydrocarbon and deuterocarbon were found to be identical. As shown in Table I, a small but consistently lower value for the deuteroparaffin (by as much as 16%) is often found when the total transition enthalpies (pretransition + melt) were compared. Numerous reevaluations of these enthalpies from scans at 0.5 °C/min indicate, however, that this slight difference may not be statistically significant. Using the calorimetric data to determine the transition enthalpy per methylene segment, a value of 920 cal/mol CH_2 is found for the alkane series compared to the theoretical value 984 cal/mol CH_2 for the melting enthalpy of polyethylene.[27]

Binary Solids. The binary phase diagram for n-$C_{36}D_{74}$/n-$C_{36}H_{74}$ has been published before[11,14] and shown to be nearly ideal in its melting behavior. Sampling at a finer concentration interval, we find the same result for samples heated 1 deg/min or 5 deg/min (Figure 3a) and the partial concentration range for which the orthorhombic to hexagonal pretransition exists is also apparent. When the samples are cooled from the melt at 1 deg/min, a complete concentration series can be seen for the premelt transition (Figure 3b). Use of ideal solution theory[21] (eq 1) to calculate the melting line fits the experimental data in both diagrams. Similar results are obtained for the n-$C_{30}D_{62}$/n-$C_{30}H_{62}$ binary solids which were also scanned at 1 deg/min (Figure 3c). It is important to note here that the temperature dependence of the solid–solid phase transition is linear with concentration. The same observation is made with the n-$C_{32}D_{66}$/n-$C_{32}H_{66}$ pair (Figure 3d). This is contrasted with phase diagrams for n-paraffin binaries where the components differ in chain length.[18] In this case, the premelt "rotator" transition temperature is nonlinear with concentration and, therefore, is nonideal. Phase diagrams for similar binaries of shorter chain n-alkanes also exhibit similar ideal behavior (Figure 3, parts e–g).

Within the precision of a and b unit cell axis measurements from $hk0$ electron diffraction patterns from samples calibrated with an internal gold standard, it is not possible to detect any changes at room temperature in these values with concentration for n-$C_{36}D_{74}$/n-$C_{36}H_{74}$ binaries. If, however, these solids are heated to 68 °C, the perdeuteroparaffin has a significantly larger a/b axial ratio than its perprotonated analogue, and this ratio appears to change smoothly with concentration (Figure 4a). Seven representative binary solids were also heated toward the melting point and $hk0$ diffraction patterns taken from single crystals at intermediate temperatures. Although there is some scatter in the values (due to local crystal bending, etc.), it is apparent that the axial ratios for n-$C_{36}D_{74}$-rich samples expand gradually with increasing temperature to reach a maximum $a/b \simeq 1.68$ for pure deuterocarbon. The n-$C_{36}H_{74}$-rich samples, for which the conversion to a hexagonal chain packing is quite abrupt, reaches the limit $a/b = 1.73$ for pure hydrocarbon. For corresponding linear chains, which both transform to the hexagonal layer packing, e.g. n-$C_{32}D_{66}$ and n-$C_{32}H_{66}$ (Figure 5), the respective a/b axial ratios for both are found to undergo the abrupt change at the transition temperature. Below this transition, the expansion of axial ratio with concentration is very smooth for samples held at elevated temperature (Figure 4b).

Discussion

Solid solutions formed from equal chain lengths of n-paraffins and their perdeuterated analogues are well explained by ideal solution theory. This is evident from the fit of experimental melting lines by Raoult's law (eq 1). Such behavior is also a feature of other n-paraffin solid solutions composed of different chain length components within the molecular volume difference stabilized in a mixed lamellar packing.[16] As proposed by Stehling et al.[11] (and shown in Table I), the solid solutions represent a comixture of two species with nearly identical enthalpies of fusion. Thus, different entropic contributions apparently account for the melting point difference of the pure components. Similar melting point changes are also exhibited by deuterium-substituted 1,2-diacyllecithins.[28] For lecithin bilayer vesicles in aqueous suspension,[29] the order of the gel to liquid crystal transition is changed with deuterium substitution.

It is also significant that a molecular volume effect can be detected in these phase diagrams from the appearance

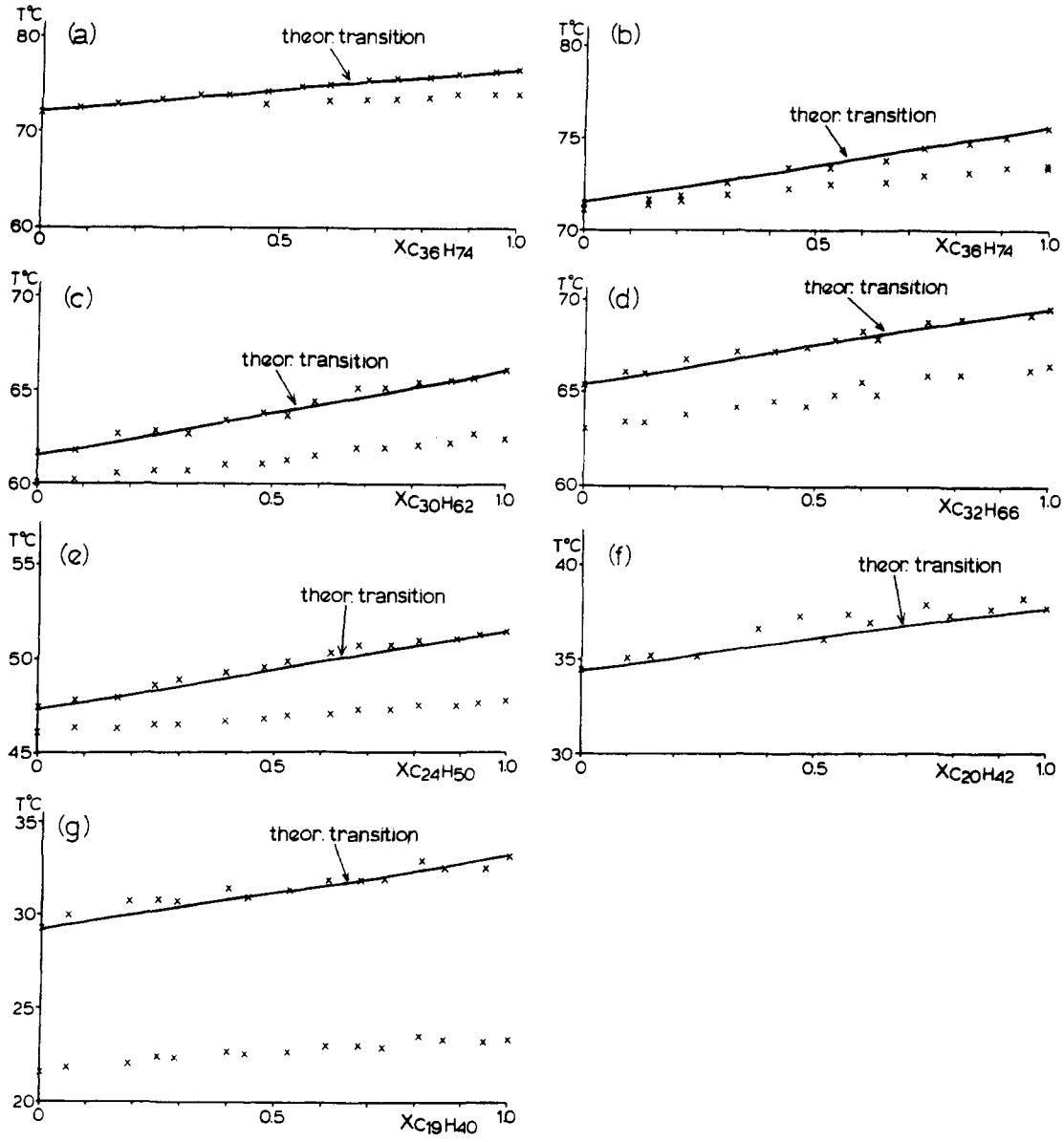

Figure 3. Binary phase diagrams for *n*-perdeuteroparaffin/*n*-paraffin combinations. The melt transition line calculated from eq 1 are compared to the experimental data: (a) n-$C_{36}D_{74}/n$-$C_{36}H_{74}$, heated 5 deg/min (a similar curve also found at 1 deg/min); (b) n-$C_{36}D_{74}/n$-$C_{36}H_{74}$, cooled 1 deg/min; (c) n-$C_{30}D_{62}/n$-$C_{30}H_{62}$, heated 1 deg/min; (d) n-$C_{32}D_{66}/n$-$C_{32}H_{66}$, heated 5 deg/min; (e) n-$C_{24}D_{50}/n$-$C_{24}H_{50}$, heated 5 deg/min; (f) n-$C_{20}D_{42}/n$-$C_{20}H_{46}$, heated 5 deg/min; (g) n-$C_{19}D_{40}/n$-$C_{19}H_{40}$, heated 5 deg/min.

of the premelt transition curve. For *n*-paraffin solid solutions comprised of unequal chain lengths,[16] the transition from the orthorhombic to hexagonal chain packing is not a linear function of concentration. The deuterocarbon/hydrocarbon combinations of like chain length, on the other hand, lead to a quite linear curve for this transition. A recent discussion[30] of Flory–Huggins theory for chemically identical species has shown how these volume differences alone can account for such nonideal behavior. Since the volume difference between hydrocarbon and deuterocarbon of the same chain length lengths is very small, e.g. 0.4% difference,[15] the linearity of the pretransition curves show that the two components apparently form an ideal solution in the crystalline solid state for all concentrations. If this is true, one must conclude that the dispersive interactions between these chemically unlike molecules are nearly the same as those between chemically identical species. The postulate of similar dispersion forces can be supported by the experimentally observed linear relationship found for melting point difference vs the hydrocarbon melting point over a very large molecular weight range.[25] As also stated by Grigor and Steele,[26] this is required by the observed adherence to the law of corresponding states.[31] That is to say, the intermolecular potential energy for the respective classes of molecules must have the same analytical forms, although the constants used for the empirical Lennard-Jones potential may be slightly different, as indicated by the small difference in potential well depths for the two molecular species.[25] (A near identity of these constants had also been assumed earlier in a calculation of methylene deformation frequencies.[32])

Thus, although perdeuteration lowers the temperature of a phase transition for an alkane C_nH_{2n+2}, the characteristics of the transition remain the same. For example, the lattice expansion found for even *n*-paraffins above and below the occurrence of the "rotator" phase can be schematized as in Figure 6. Paraffins of all chain lengths expand slightly as they are heated toward the melting point and a plot of this initial limit is found to be nearly constant over all chain lengths from n-$C_{28}H_{58}$ to n-$C_{82}H_{166}$ (Figure 7). At this point, the intensity distribution of the electron diffraction pattern still resembles Figure 1a. Those members which transform to a "rotator" packing will then

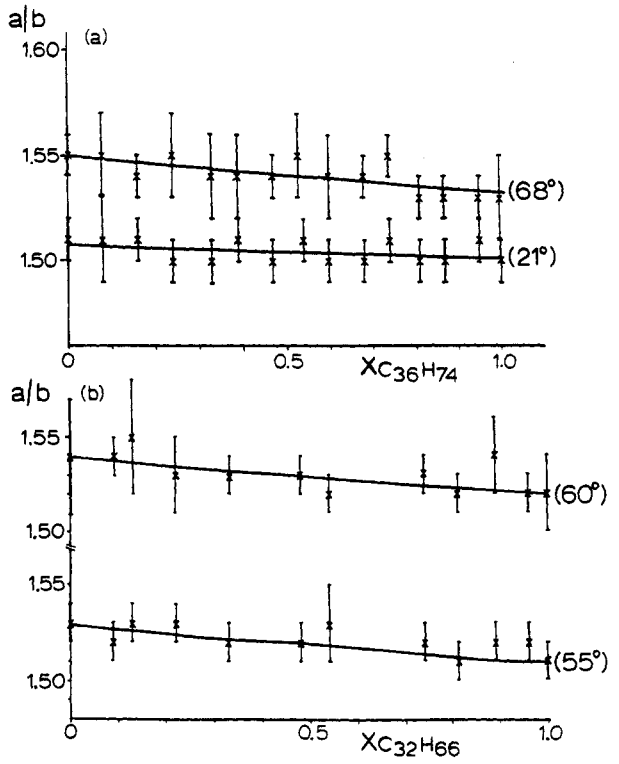

Figure 4. Lattice ratios for binary comixtures of paraffins with their perdeuterated analogs: (a) n-$C_{36}D_{74}/n$-$C_{36}H_{74}$; (b) n-$C_{32}D_{66}/n$-$C_{32}H_{66}$.

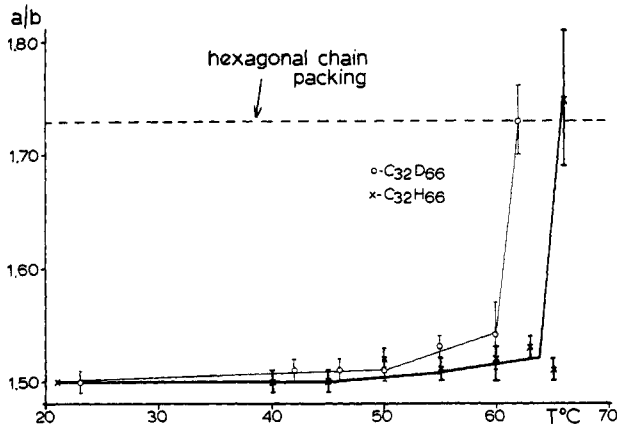

Figure 5. Comparison of a/b values for heated samples of n-$C_{32}D_{66}$ and n-$C_{32}H_{66}$. These measurements were made from single-crystal electron diffraction patterns.

abruptly jump to the $a/b = \sqrt{3}$ value for this disordered chain packing. Here the symmetry and intensity distribution of the diffraction pattern changes. For n-$C_{32}D_{66}$, which also has a true "rotator" phase, the analogy with its perprotonated analogue is exact with the same a/b dimensional limits reached during heating (Figure 5). The lattice expansion of binary solids of the like chain lengths is also continuous with concentration (Figure 4b), indicating an intimate comixing of components.

At first, the behavior of n-$C_{36}D_{74}$ seems to be somewhat anomalous, but can be shown to fulfill the expectations of a paraffin which lies on a chain length boundary where the true "rotator" phase disappears. The lateral expansion of the crystalline lattice appears to be continuous with heating but with abrupt transition near the melting point to a value $a/b = 1.68 \pm 0.03$ (Figure 7) which is not quite the ratio found for the true hexagonal phase. The diffraction pattern (Figure 8a) in a projection down the

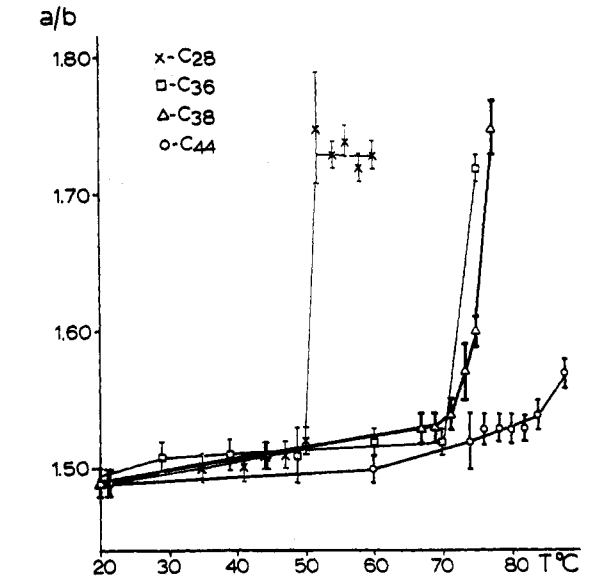

Figure 6. Change of axial ratio a/b with temperature for n-paraffins. Paraffins up to n-$C_{38}H_{78}$ undergo a transition to the "rotator" phase before melting and hence $a/b = 1.73$ is reached. These plots are representative of heating experiments carried out for materials in a chain length series from n-$C_{28}H_{58}$ to n-$C_{82}H_{166}$, where paraffin chains starting with n-$C_{40}H_{82}$ and longer do not form a hexagonal "rotator" phase before melting.

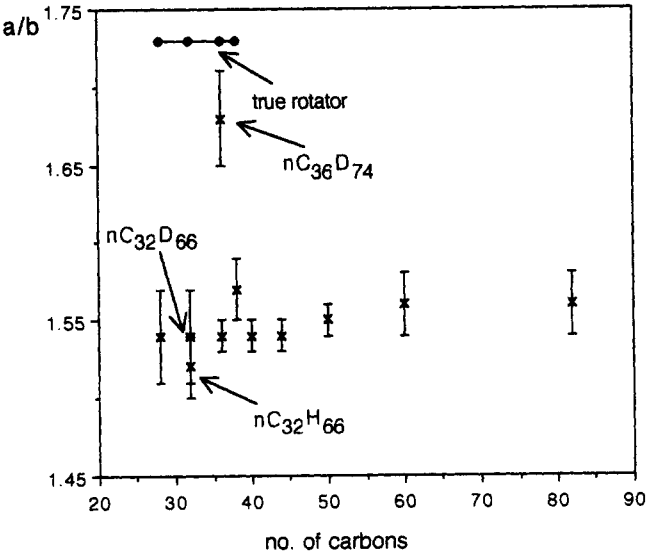

Figure 7. Plot of lattice expansion limits for heated even n-paraffins. All paraffins expand to a value $a/b \simeq 1.55$ but only those chain length $n \leq 38$ reach the second limit $a/b = 1.73$ characteristic of the "rotator" phase. For deuteroparaffins, the behavior of n-$C_{32}D_{66}$ is identical to these paraffins whereas n-$C_{36}D_{66}$ only expands to the rotationally disordered orthorhombic packing described by Ungar.[33]

chain axes shows that the disordered structure is a centered orthorhombic structure, probably corresponding to the nonhexagonal high temperature layer packing proposed by Ungar.[33] On the other hand, the major consequence of heating any crystalline paraffin or deuteroparaffin is to disorder the lamellar interfaces, as found in the electron diffraction study of epitaxially oriented n-$C_{36}D_{74}$ samples (Figure 8, parts b–d). Thus, the disorder mechanism is exactly the same found in a similar study of n-$C_{36}H_{74}$.[34] (Vibrational spectroscopic studies also demonstrate that this thermally induced lamellar disorder is common to all paraffins irrespective of chain length.[35]) Although somewhat noisy, plots of axial ratio for binary combinations of a n-$C_{36}D_{74}/n$-$C_{36}H_{74}$ (Figure 4a) again indicate that the

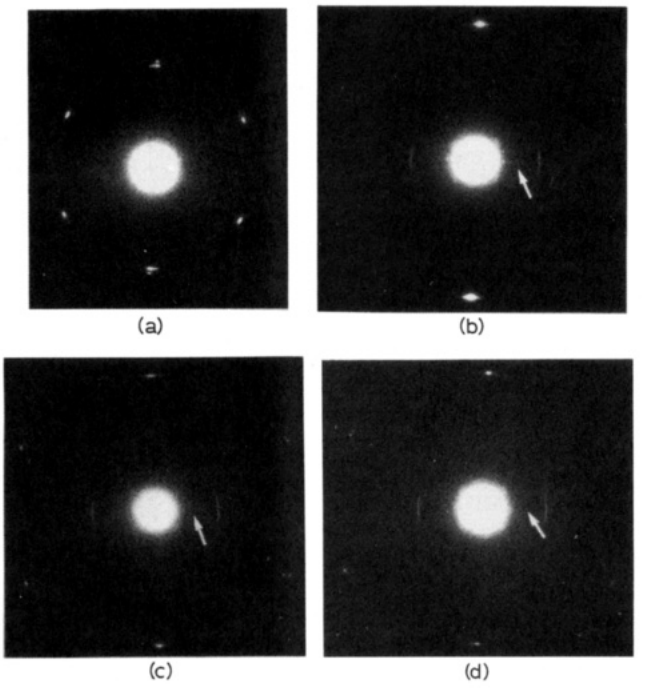

Figure 8. Electron diffraction patterns of heated n-$C_{36}D_{74}$: (a) view down chain axes at 70 °C. Although the structure is rotationally disordered, the a/b ratio does not equal $\sqrt{3}$. Epitaxially oriented sample are shown in parts b–d: (b) at 42 °C, (c) at 61 °C, and (d) at 65 °C. Note the attenuation of lamellar reflections denoting the onset of interfacial disorder between lamellae. (The pattern in a is shown at a different scale than those in b, c, and d.)

components are intimately mixed.

To summarize the above results, deuteroparaffins are found to have structural properties quite similar to the parent n-paraffins of the same chain length with very little difference in molecular volume. The melting properties have been found to be strictly comparable from the single carbon to infinite carbon chains,[25] indicating that the analytical expressions for internal energy are similar. Phase diagrams of binary solids comprised of equal chain length pairs further support this postulate of very similar intermolecular dispersion forces.

Acknowledgment. Research supported by NSF Grant No. DMR86-10783. I thank Dr. Robert G. Snyder for the gift of some of the perdeuterated paraffins used in this study and also for fruitful discussions of this work. Also thanks are due to Dr. J. R. Fryer for a gift of n-$C_{82}H_{166}$.

References and Notes

(1) Zaccai, G.; Büldt, G.; Seelig, A.; Seelig, J. *J. Mol. Biol.* **1979**, *134*, 693.
(2) Büldt, G.; Gally, U.; Seelig, J.; Zaccai, G. *J. Mol. Biol.* **1979**, *134*, 673.
(3) Maroncelli, M.; Strauss, H. L.; Snyder, R. G. *J. Chem. Phys.* **1985**, *82*, 2811.
(4) Marconcelli, M.; Strauss, H. L.; Snyder, R. G. *J. Phys. Chem.* **1985**, *89*, 5260.
(5) Tasumi, M.; Krimm, S. *J. Chem. Phys.* **1967**, *46*, 755.
(6) Krimm, S.; Cheam, T. C. *Faraday Discuss Chem. Soc.* **1979**, *68*, 244.
(7) Spells, S. *Polymer* **1985**, *26*, 1921.
(8) Wignall, G. D.; Mandelkern, L.; Edwards, C.; Glotin, M. *J. Polym. Sci., Polym. Phys. Ed.* **1982**, *20*, 245.
(9) Spells, S. J.; Sadler, D. M. *Polymer* **1984**, *25*, 739.
(10) Yang, H.; Stein, R. S.; Han, C. C.; Bauer, B. J.; Kramer, E. J. *Polym. Commun.* **1986**, *27*, 132.
(11) Stehling, F. C.; Ergos, F.; Mandelkern, L. *Macromolecules* **1971**, *4*, 672.
(12) Buckingham, A. D.; Hentschel, H. G. E. *J. Polym. Sci., Polym. Phys. Ed.* **1980**, *18*, 853.
(13) Krimm, S.; Ching, J. H. C. *Macromolecules* **1972**, *5*, 209.
(14) English, A. D.; Smith, P.; Axelson, D. E. *Polymer* **1985**, *26*, 1523.
(15) Bates, F. S.; Fehers, L. J., Wignall, G. D. *Macromolecules* **1988**, *21*, 1086.
(16) Dorset, D. L. *Macromolecules* **1990**, *23*, 623.
(17) Broadhurst, M. G. *J. Chem. Phys.* **1962**, *36*, 2578.
(18) Dorset, D. L. *J. Electron Microsc. Techn.* **1985**, *2*, 89.
(19) Dorset, D. L. In *Comprehensive Polymer Science*; Vol. 1 (*Polymer Characterization*), 1989, Booth, C., Price, C., Eds.; Pergamon: Oxford, p 651.
(20) Broadhurst, M. G. *J. Res. Natl. Bur. Stand.* **1962**, *66A*, 241.
(21) Lee, A. G. *Biochim. Biophys. Acta* **1977**, *472*, 285.
(22) Dorset, D. L. *Acta Crystallogr.* **1976**, *A32*, 207.
(23) Dorset, D. L. *J. Polym. Sci., Polym. Phys. Ed.* **1986**, *24*, 79.
(24) Ungar, G.; Keller, A. *Colloid Polym. Sci.* **1979**, *257*, 90.
(25) Dorset, D. L.; Strauss, H. L.; Snyder, R. G. *J. Phys. Chem.* **1991**, *95*, 938.
(26) Grigor, A. F.; Steele, W. A. *J. Chem. Phys.* **1968**, *48*, 1038.
(27) Dollhopf, W.; Grossmann, H. P.; Leute, N. *Colloid Polym. Sci.* **1981**, *259*, 267.
(28) Casal, H. L.; Mantsch, H. H.; Cameron, D. G.; Gaber, B. P. *Chem. Phys. Lipids* **1883**, *33*, 109.
(29) Guard-Friar, D.; Chen, C.-H.; Engle, A. S. *J. Phys. Chem.* **1985**, *89*, 1810.
(30) Mandelkern, L.; Smith, F. L.; Chan, E. K. *Macromolecules* **1989**, *22*, 2663.
(31) Beattie, J. A.; Stockmeyer, W. H. In *A treatise on Physical Chemistry, 3rd ed.*; Taylor, H. S.; Glasstone, S. eds.; D. van Nostrand: New York, 1952; Vol II (*States of Matter*), p 342.
(32) Stein, R. S. *J. Chem. Phys.* **1955**, *23*, 734.
(33) Ungar, G.; Masic, N. *J. Phys. Chem.* **1985**, *89*, 1036.
(34) Dorset, D. L.; Moss, B.; Wittmann, J.-C.; Lotz, B. *Proc. Nat. Acad. Sci. USA* **1984**, *81*, 1913.
(35) Kim, Y.; Strauss, H. L.; Snyder, R. G. *J. Phys. Chem.* **1989**, *93*, 7520.
(36) Nyburg, S. C.; Potworowski, J. A. *Acta Crystallogr.* **1973**, *1329*, 347.

Registry No. $C_{19}H_{40}$, 629-92-5; $C_{19}D_{40}$, 39756-36-0; $C_{20}H_{42}$, 112-95-8; $C_{20}D_{42}$, 62369-67-9; $C_{24}H_{50}$, 646-31-1; $C_{24}D_{50}$, 16416-32-3; $C_{30}H_{62}$, 638-68-6; $C_{30}D_{62}$, 93952-07-9; $C_{32}H_{66}$, 544-85-4; $C_{32}D_{66}$, 62369-68-0; $C_{36}H_{74}$, 630-06-8; $C_{36}D_{74}$, 16416-34-5; polyethylene, 9001-88-4.